

Supplemental Figures

Inferring disease progressive stages in single-cell transcriptomics using a weakly-supervised deep learning approach

Fabien Wehbe, Levi Adams, Jordan Babadoudou, Samantha Yuen, Yoon-Seong Kim, and Yoshiaki

Tanaka

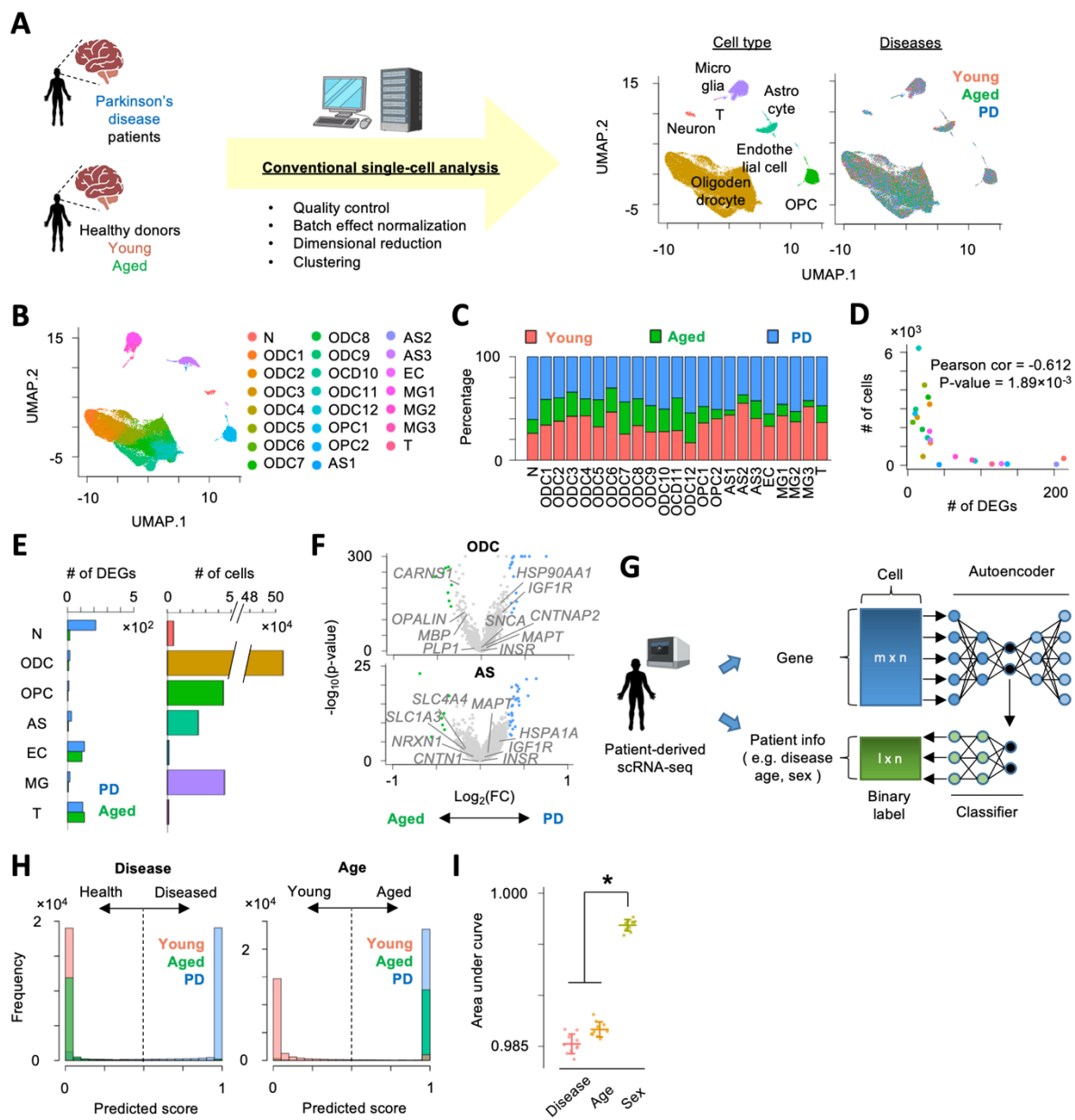
Table of Contents

Supplemental Figure 1. Conventional scRNA-seq analysis and application of supervised learning model to single-cell transcriptome profiles of Parkinson's disease patients

Supplemental Figure 2. Application of weakly-supervised deep learning model to Parkinson's disease patient-derived single-cell transcriptome profiles

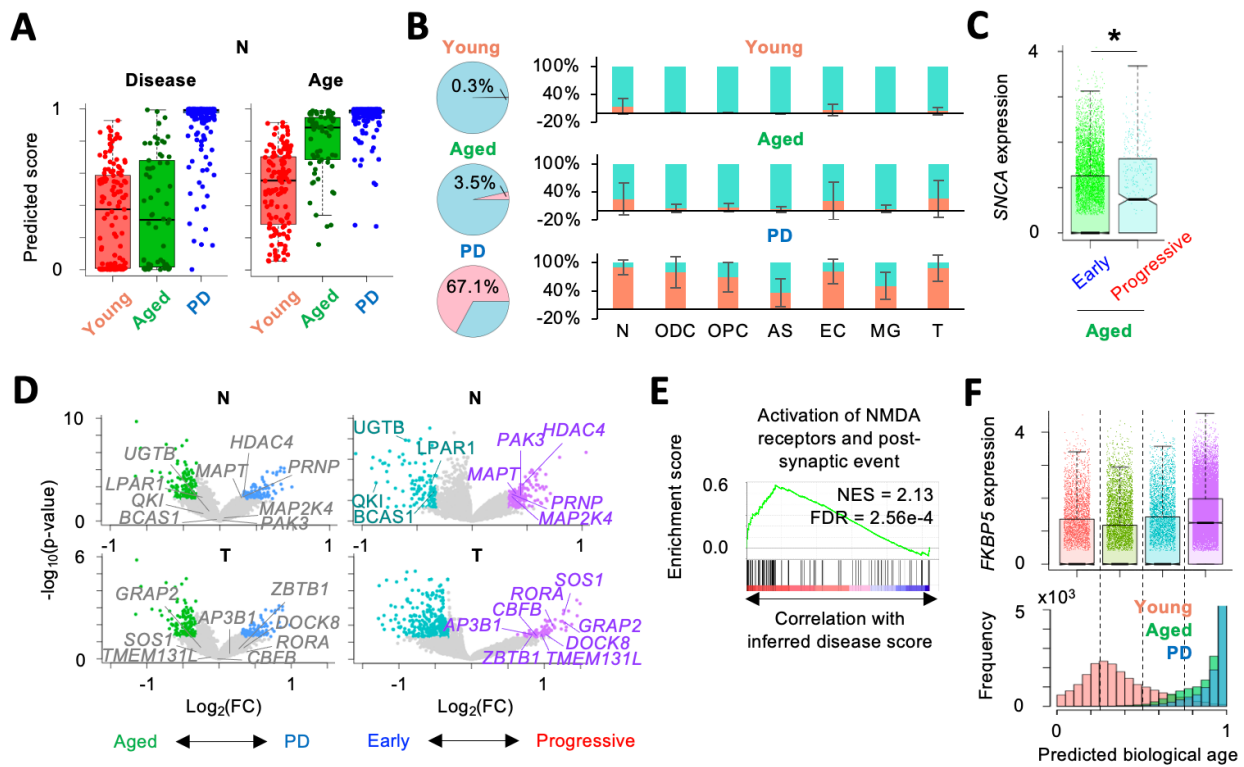
Supplemental Figure 3. Application of pre-trained weakly-supervised models to other independent single-cell datasets

Supplemental Figure 4. Inference of CD4⁺ and CD8⁺ CAR-T cell activation dynamics to neuroblastoma



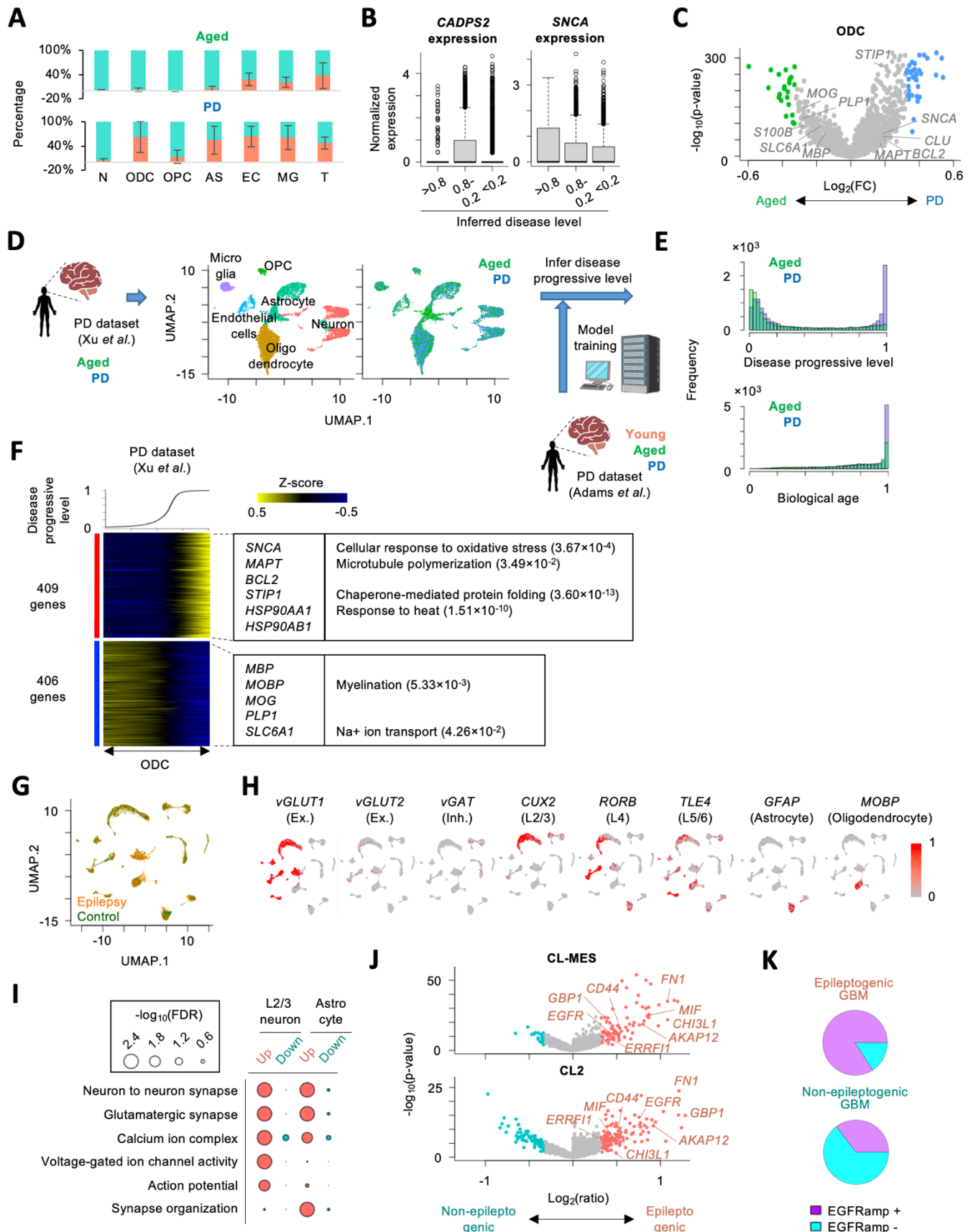
Supplemental Figure 1. Conventional scRNA-seq analysis and application of supervised learning model to single-cell transcriptome profiles of Parkinson's disease patients

A. Conventional single-cell analysis clusters cells into cell types, but not into disease. **B.** UMAP plots of single cells colored by clusters. **C.** Composition of origins of cells in each cluster. **D.** Inverse correlation between the number of differentially-expressed genes and the number of cells in each cluster. **E.** Comparison between (left) the number of differentially-expressed genes (DEGs) between Parkinson's disease patient and age-matched healthy donor and (right) the number of cells in each cell type. **F.** Volcano plots showing differential expression between PD patients and age-matched donors **G.** Supervised deep learning model to discriminate diseased and healthy cells. **H.** Histogram of prediction score (output of deep learning model) of disease and age. **I.** Comparison of area under curve in the prediction of disease, age, and sex. Error bar represents standard deviation ($n=10$). * $p<0.05$ by two-sided *t*-test.



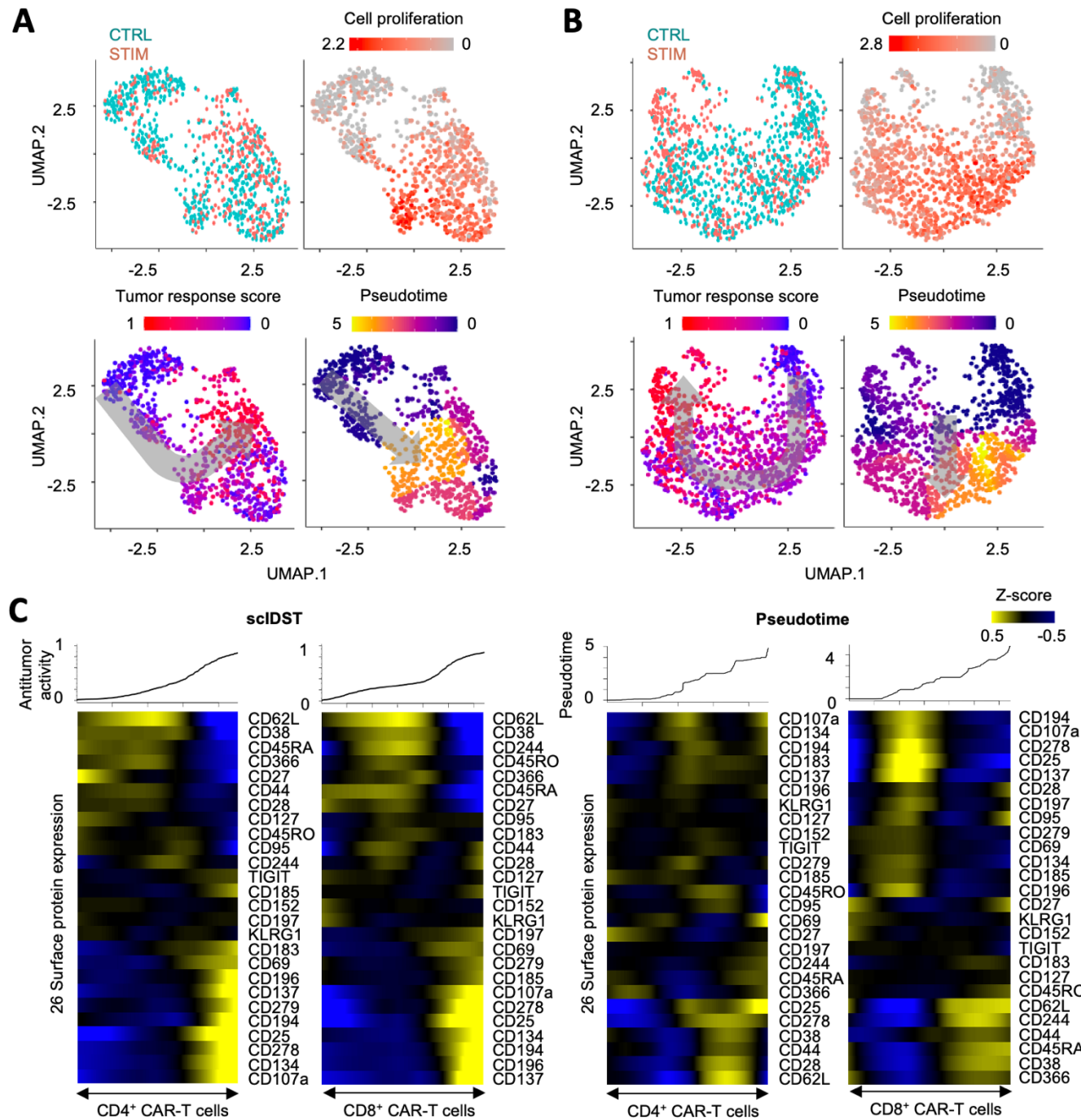
Supplemental Figure 2. Application of weakly-supervised deep learning model to Parkinson's disease patient-derived single-cell transcriptome profiles

A. Comparison of the inferred disease progressive levels and biological ages in neurons across healthy young, aged donors, and Parkinson's disease patients. **B.** Pie charts showing frequency of disease progressive cells. The frequency in each cell type is shown in right panel. Error bars represent standard deviation. **C.** Comparison of SNCA expression between early/healthy and disease progressive cells in aged brain. **D.** Volcano plot showing differential expression in neurons and T cells (left) between PD patients and healthy aged donors and (right) between disease progressive stage and early/heathy stage. **E.** Activation of NMDA receptor pathway over the inferred disease process. **F.** Correlation between predicted biological age and *FKBP5* expression. Cells are separated into four groups by predicted biological age. Comparison of *FKBP5* expression across four groups and Histogram of predicted biological age are shown in top and bottom, respectively.



Supplemental Figure 3. Application of pre-trained weakly-supervised models to other independent single-cell datasets

A. Frequency of the inferred disease progressive cells in each cell type of Smajic *et al.* dataset. Error bars represent standard deviation. **B.** Comparison of (L) CADPS2 and (R) SNCA expression across three groups that were classified by the inferred disease progressive level. **C.** Volcano plot showing differential expression in oligodendrocyte between PD patients and healthy aged donors in Smajic *et al.* dataset. **D.** Strategy to estimate Parkinson's disease progressive level by the pre-trained model in another scRNA-seq dataset from different brain area. **E.** Histogram of predicted score of disease progressive level and biological age. **F.** Heatmap showing genes, whose expression is highly correlated with inferred disease progressive score (Genes with Pearson correlation > 0.1). Oligodendrocyte cells are sorted by the disease progressive score. Heatmap color represents z-score-normalized gene expression. Representative genes and GO terms are shown in right panel. Statistical significance of GO terms is shown by false discovery rate. **G.** UMAP plot of single cells colored by epilepsy patients (orange) and healthy control donors (darkgreen). **H.** UMAP plot showing representative cell type-specific gene expression in epilepsy patients and healthy donors-derived scRNA-seq dataset. **I.** Representative GO terms overrepresented in differentially-expressed genes between epileptic and non-epileptic cells. Circle size represents $-\log_{10}(\text{FDR})$. **J.** Volcano plots showing differential expression between epileptogenic and non-epileptogenic GBM cells in CL-MES and CL2 cluster. Significantly-upregulated ERK1/2 cascade-related genes are also shown. **K.** Pie chart showing ratio of cells with EGFR amplification in the inferred epileptogenic and non-epileptogenic GBM cells.



Supplemental Figure 4. Inference of CD4⁺ and CD8⁺ CAR-T cell activation dynamics to neuroblastoma

A-B. UMAP plots of **(A)** CD4⁺ and **(B)** CD8⁺ individual CAR-T cells colored by the stimulation conditions (top left), cell proliferation-related gene expression (top right), the inferred antitumor activity (bottom left), and pseudotime (bottom right). **C.** Heatmap showing 26 surface protein expression dynamics in CD4⁺ and CD8⁺ CAR-T cells. CAR-T cells were sorted by (left) scIDST or (right) pseudotime. Heatmap color represents z-score-normalized protein expression.